Taylor & Francis
Taylor & Francis Group

Inhalation Toxicology

International Forum for Respiratory Research

ISSN: 0895-8378 (Print) 1091-7691 (Online) Journal homepage: https://www.tandfonline.com/loi/iiht20

The Biopersistence of Canadian Chrysotile Asbestos Following Inhalation

David M. Bernstein, Rick Rogers & Paul Smith

To cite this article: David M. Bernstein, Rick Rogers & Paul Smith (2003) The Biopersistence of Canadian Chrysotile Asbestos Following Inhalation, Inhalation Toxicology, 15:13, 1247-1274, DOI: 10.1080/08958370390241713

To link to this article: https://doi.org/10.1080/08958370390241713

Inhalation Toxicology, 15:1247–1274, 2003

ISSN: 0895-8378 print / 1091-7691 online
DOI: 10.1080/08958370390241713

Taylor & Francis
healthsciences

THE BIOPERSISTENCE OF CANADIAN CHRYSOTILE ASBESTOS FOLLOWING INHALATION

David M. Bernstein

Consultant in Toxicology, Geneva, Switzerland

Rick Rogers

Rogers Imaging Corporation, Needham, Massachusetts, USA

Paul Smith

Research & Consulting Company Ltd., Füllinsdorf, Switzerland

Chrysotile asbestos is often included with other asbestos materials in evaluation and classification. However, chrysotile is a serpentine with markedly different physical and chemical characteristics in comparison to amphiboles (e.g., crocidolite, amosite, tremolite). In contrast to amphiboles, which are solid, rodlike fibers, chrysotile is composed like a rope of many fine fibrils, which tend to unwind. In order to quantify the dynamics and rate by which chrysotile is removed from the lung, the biopersistence of a sample of commercial chrysotile from the Eastern Townships area of Quebec, Canada, labeled QS Grade 3-F, which is the longest commercial grade intended for textile use, was studied. As the long fibers have been shown to have the greatest potential for pathogenicity, the chrysotile samples were specifically chosen to have more than 200 fibers/cm^3 longer than 20 μm present in the exposure aerosol. This publication presents the results of this study through 3 mo postexposure. The study design included: (1) Fiber clearance (lung digestions): At 1 day, 2 days, 7 days, 14 days, 1 mo, 3 mo, and 12 mo (to be reported) following a 5-day (6 h/day) inhalation exposure, the lungs from groups of animals were digested by low-temperature plasma ashing and subsequently analyzed by transmission electron microscopy for total chrysotile fibers number in the lungs and chrysotile fiber size (length and diameter) distribution in the lungs. (2) Fiber distribution (confocal microscopy): This procedure was included in order to identify the location of the fibers in the lung. At 1 day, 2 days, 7 days, 14 days, 1 month, and 3 months (to be reported) postexposure, the lungs from groups of animals were analyzed by confocal microscopy to determine the anatomic fate, orientation, and distribution of the retained chrysotile fibrils deposited on airways and in the parenchymal region. Chrysotile was found to be rapidly removed from the lung. Fibers longer than 20 μm were cleared with $T_{1/2}$ = 16 days, most likely by dissolution and disintegration into shorter fibers. The shorter fibers were also rapidly cleared from the lung, with fibers 5–20 μm clearing even faster ($T_{1/2}$ = 29.4 days) than those <5 μm in length. The fibers <5 μm in length cleared at a rate ($T_{1/2}$ = 107 days) that is within the range of clearance for insoluble nuisance dusts. The breaking apart of the longer fibers would be expected to increase the short fiber pool and therefore could account for this difference in clearance rates. The short fibers were not found clumped together but appeared as sepa-

Received 14 May 2003; accepted 23 June 2003.

This study was supported by grants from the Government of Québec and The Asbestos Institute, Montréal, Québec, Canada.

Address correspondence to Dr. David Bernstein, Consultant in Toxicology, 40 chemin de la Petite-Boissière, 1208 Geneva, Switzerland. E-mail: davidb@itox.ch

rate, fine fibrils, occasionally unwound at one end. Short free fibers appeared in the corners of alveolar septa, and fibers or their fragments were found within alveolar macrophages. The same was true of fibers in lymphatics, as they appeared free or within phagocytic lymphocytes. Neutrophil-mediated inflammatory response did not occur in the presence of chrysotile fibers at the time points examined. Taken in context with the scientific literature to date, this report provides new robust data that clearly support the difference seen epidemiologically between chrysotile and amphibole asbestos.

Asbestos has been implicated in disease through both epidemiological and animal toxicology studies. However, the serpentine asbestos chrysotile is very different chemically and mineralogically from amphibole asbestos such as amosite, crocidolite, or tremolite. This has resulted in some researchers suggesting that chrysotile may not be of the same potency as the amphiboles and may clear faster from the lung (Howard, 1984; Churg & DePaoli, 1988; Mossman et al., 1990; Morgan, 1994; Churg, 1994; McDonald, 1997, 1998; Rodelsperger et al., 1999; McDonald et al., 1999).

To examine the dynamics and rate of clearance of chrysotile from the lung, an inhalation biopersistence study in the rat was initiated using a sample of commercial chrysotile from the Eastern Townships area of Quebec, Canada. The protocol for this study was designed to meet the specific recommendations of the European Commission (EC) Interim Protocol for the Inhalation Biopersistence of synthetic mineral fibers (Bernstein & Riego-Sintes, 1999). For synthetic mineral fibers, the biopersistence of the fibers longer than 20 μm has been found to be related to their potential to cause disease (Bernstein et al., 2001). As described later, the specifications in the protocol for counting and sizing the fibers were modified to accommodate the finer dimensions of the chrysotile fibers in comparison to mineral fibers. In addition, the disposition of fibers within the lung was also determined using confocal microscopy. This article presents the results through 90 days after cessation of exposure. A subsequent article will present further results through 1 yr after cessation of exposure.

The exposure and in-life phases of the study were performed at the Research and Consulting Company Ltd., Füllinsdorf, Switzerland. Fiber counting and sizing was performed under subcontract to RCC at Gesellschaft für Schadstoffmessung und Auftragsanalytik (GSA), Neuss, Germany. The confocal microscopy analysis was performed by Rogers Imaging Corporation, Needham, MA.

METHODS

Chrysotile Sample Characteristics

The chrysotile fiber is monoclinic in crystalline structure and has a unique rolled structure described later. The chrysotile used in this study was labeled QS Grade 3-F on the Canadian Quebec Screening Scale (QSS) and is a commercial textile grade that is the longest grade intended for textile use (Cossette & Delvaux, 1979).

The chemical composition and the structure of chrysotile are markedly different from that of amphiboles such as tremolite or amosite (Hodgson, 1979).

Table 1 summarizes the chemical composition of typical serpentine and amphibole asbestos. The chemistry of chrysotile is composed of a silicate sheet of composition $(Si_2O_5)_n^{2n-}$, in which three of the O atoms in each tetrahedron are shared with adjacent tetrahedra and a nonsilicate sheet of composition $[Mg_3O_2(OH)_4]_n^{2n+}$. In chrysotile the distances between apical oxygens in a regular (idealized) silicate layer are shorter (0.305 nm) than the O–O distances in the ideal Mg-containing layer (0.342 nm), which may account for the curling of the layers that results in the rolling up like a carpet to form concentric hollow cylinders (Skinner et al., 1988). This structure is illustrated in Figure 1 (adapted from Skinner et al., 1988) and transmission electron micrographs of chrysotile are shown in Figure 2 (Kiyohara, 1991). The Mg molecule is on the outside of the curl and is thus exposed to the surrounding environment.

In contrast, with amphiboles such as tremolite, the basic structure is in the form of an I-beam with corner-linked $(SiO_4)^{4-}$ tetrahedra linked together in a double-tetrahedral chain that sandwiches a layer with the Ca_2Mg_5. In contrast to chrysotile, with tremolite, the Mg is locked within the I-beam structure. This is illustrated in Figure 3.

Experimental Design

The results of the lung digestion measurements through 3 mo after cessation of exposure and of the confocal microscopy examination through 1 mo after cessation of exposure are presented. Following termination of the

TABLE 1. Typical chemical composition (percent)

Compound	Chrysotile[a]	Tremolite[b]	Amosite[c]
SiO_2	40.6	55.10	49.70
Al_2O_3	0.7	1.14	0.40
Fe_2O_3	2.3	0.32	0.03
FeO	1.3	2.00	39.70
MnO	—	0.10	0.22
MgO	39.8	25.65	6.44
CaO	0.6	11.45	1.04
K_2O	0.2	0.29	0.63
Na_2O	—	0.14	0.09
H_2O^+	—	3.52	1.83
H_2	—	0.16	0.09
CO_2	0.5	0.06	0.09
Ignition loss	14.0	—	—
Total	100	99.93	100.26

[a]Typical chemical analysis of Canadian chrysotile from the Quebec Eastern Townships (LAB Chrysotile, Inc., Quebec, Canada).

Hodgson (1979, pp. 80–81).

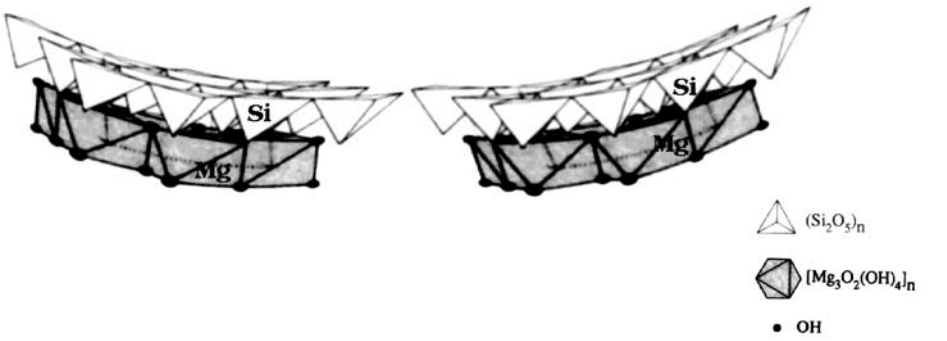

FIGURE 1. Schematic representation of the chemical structure of chrysotile showing the Mg molecule is on the outside of the curl. Adapted from Skinner et al. (1988).

study at 12 mo postexposure the remaining results will be presented in a separate publication.

The experimental design of the in-life and biopersistence analysis has been presented in detail previously (Bernstein et al., 1994) and is summarized next. In particular, details of the counting and sizing procedures are reiterated as these are considered essential to the successful interpretation of these studies.

Animal exposure Groups of 56 weanling (approximately 9 wk old) male Wistar rats (specific-pathogen-free quality) were exposed by flow-past nose-only exposure to a target fiber aerosol concentration of 200 fibers, L > 20 μm/cm^3, for 6 h/day for a period of 5 consecutive days. This concentration corresponded to two times that required by the EC Biopersistence Protocol in order to assure that there was no question of sufficient long fiber exposure. In addition, a negative control group was exposed in a similar fashion to filtered air. Wistar rats (HanBrl:WIST, SPF), obtained from RCC Ltd., Biotechnology and Animal Breeding Division, CH-4414 Füllinsdorf, Switzerland, were used.

Exposure system The fiber was prepared for the exposures prior to the technical trials by grinding it in a Cyloctec sample mill (Tecator, Sweden),

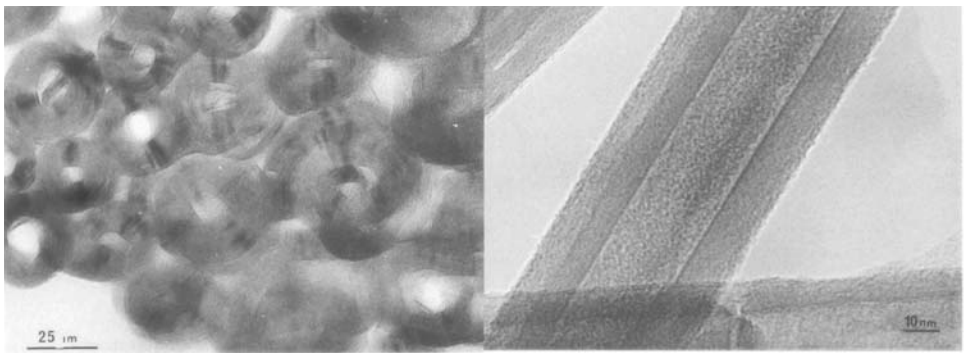

FIGURE 2. Transmission electron micrographs of chrysotile showing the curled sheetlike form of the fibers (Kiyohara, 1991).

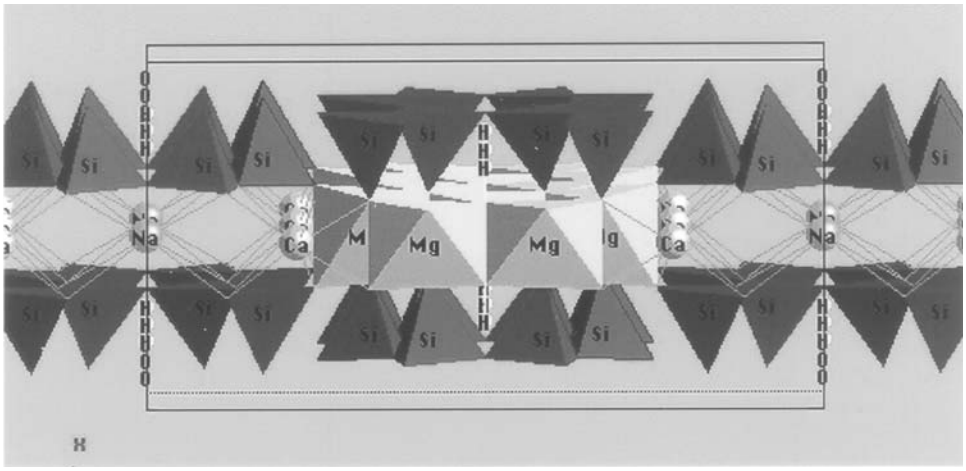

FIGURE 3. Schematic representation of the chemical structure of tremolite showing the Mg which is locked within the I-beam structure. Adapted with permission from Department of Geology and Geophysics, University of Wisconsin, Crystal Structure Movies (http://www.geology.wisc.edu).

which grinds samples by a high-speed action, rolling the sample against the inner circumference of a durable grinding surface, and then passes it through a fine mesh screen. The fiber aerosol generation system was designed to loft the bulk fibers without breaking, grinding, or contaminating the fibers (Bernstein et al., 1994). The animals were exposed by the flow-past nose/snout-only inhalation exposure system. This system was derived from Cannon et al. (1983) and is different from conventional nose-only exposure systems in that fresh fiber aerosol is supplied to each animal individually and exhaled air is immediately exhausted.

Fiber clearance At 1 day, 2 days, 7 days, 2 wk, 1 mo, 3 mo, and 12 mo (to be reported) postexposure, the lungs from groups of animals were digested by low-temperature plasma ashing and subsequently analyzed by transmission electron microscopy (at the GSA Corp.) for total chrysotile fibers number in the lungs and chrysotile fiber size (length and diameter) distribution in the lungs. This lung digestion procedure digests the entire lung with no possibility of identifying where in the lung the fibers are located.

Fiber distribution This procedure was undertaken to determine the distribution of fibers within various pulmonary compartments. At 1 day, 2 days, 7 days, 14 days, 1 mo, and 3 mo (to be reported) postexposure, the lungs from groups of animals were prepared and analyzed by confocal microscopy. The locations of chrysotile fibrils deposited on conducting airways, respiratory airways, and parenchyma was quantified.

Lung Digestion for Fiber/Particle Analysis

From five out of the seven rats per group per time point the lungs were thawed and the entire lung was prepared for analysis. The tissue was initially dehydrated by freeze drying (Edwards EF4 Modulyo freeze dryer) and dried to

constant weight to determine the dry weight of the tissue. The dry tissue was plasma ashed in a Plasma Systems 200 (Technics Plasma GmbH) multiple chamber plasma unit at 300 W for approximately 16 h. Upon removal from the ashing unit, the ash from each lung was weighed and suspended in 10 ml methanol using a low-intensity ultrasonic bath. The suspension was then transferred into a glass bottle with the combustion boat rinse and the volume made up to 20 ml. An aliquot was then removed and filtered onto a gold-coated polycarbonate filter (pore size of 0.2 μm).

Counting rules for the evaluation of air and lung samples by transmission electron microscopy All fibers visible at a magnification of 10,000× were taken in consideration. All objects seen at this magnification were sized with no lower or upper limit imposed on either length or diameter. The bivariate length and diameter was recorded individually for each object measured. Fibers were defined as any object that had an aspect ratio of at least 3:1. The diameter was determined at the greatest width of the object. All other objects were considered as nonfibrous particles.

The stopping rules for counting of each sample were defined as follows: For nonfibrous particles, the recording of particles was stopped when a total of 30 particles were recorded. For fibers, the recording was stopped when 500 fibers with length $\geqslant$5 μm, diameter $\leqslant$3 μm (often referred to as a WHO fiber; WHO, 1985) or a total of 1000 fibers and nonfibrous particles was recorded. If this number of fibers was not reached after evaluation of 0.15 mm^2 of filter surface, additional fields of view were counted until either 500 WHO fibers were reached or a total of 5 mm^2 of filter surface was evaluated, even if a total of 500 countable WHO fibers were not reached. The evaluation of short fibers (length <5 μm) was stopped when 100 short fibers were reached.

Validation

The analytical procedures used for fiber recovery (lung digestion and transmission electron microscopy) have been validated using an independent comparative analysis with confocal microscopy which is noninvasive (a cube of the lung was analyzed in three dimensions) and have been shown not to bias the size distribution or number of the measured fibers.

Confocal Imaging of Fibers and Lung Tissue

The lungs of animals designated for confocal microscopy analysis were fixed in Karnovski's fixative by gentle instillation under a pressure of 30 cm H_2O with simultaneous immersion in fixative. The trachea was then ligated and the inflated lungs were stored in the same fixative. Following fixation, apical lobes were divided into five pieces (10 mm^2 × 5 mm thick) cut parallel to the hilum, dehydrated in graded ethanolic series to absolute, stained with 0.005% Lucifer yellow, and embedded in Spurr plastic for microscopic analysis (Rogers et al., 1999). Flat surfaces were prepared from hardened plastic blocks containing embedded lung pieces.

Confocal Fiber Quantification Confocal microscopy was performed on three randomly selected animals from each time point using Sarastro 2000 (Molecular Dynamics, Inc.) laser scanning microscopes fitted with 25-mW argon-ion lasers and an upright microscope (Optiphot-2; Nikon, Inc., or Zeiss Axiophot) modified for reflected light imaging. These confocal microscopes were used to record image data in dual-channel reflected and fluorescent imaging mode. Optical bench settings for the Sarastro 2000 CLSMs were: excitation 488 nm (Lucifer yellow), emission >510 nm long-pass filter, laser power 12–15 mW, 30% transmission, photomultiplier voltage set between 500 and 800 V. Fluorescently labeled cellular constituents and reflective/refractive fibers (and particles) were imaged simultaneously with this arrangement. Each "exposure" produced two digital images in perfect register with one another.

An image recorded in either mode was a two-dimensional (x,y), 512 × 512 array of pixels, each with an intensity value from 0 to 254 gray scale units (a value of 255 indicated saturation of the intensity scale). Optical (x,y) sections, individually and in depth series, were recorded at various positions along the z axis by adjusting the stage height using stepper motors under computer control. Images and image series were analyzed and prepared for presentation by employing specialized computer software.

Images were recorded through 40× objectives. The dimensions of voxels in the recorded volume were (x, y, and z dimensions, respectively) 0.13 μm, 0.13 μm, and 0.3 μm.

Morphometric methods In the case of three-dimensional microscopical methods, strategies for specimen examination and image sampling are strongly determined by the selection of questions to be addressed. Although it was realized that questions regarding the size distribution of fibers retained within the entire lung would be more efficiently answered by the conventional ashing/electron microscopical technique, questions about the numbers (not sizes) of fibers within various anatomical compartments would be answered most effectively by confocal microscopy employing serial optical section techniques. In many instances, the true length of individual fibrils was captured within the volume recorded in serial section stacks. This occurs if the fibril profile is oriented such that two free ends are present.

Sampling Strategy for Parenchyma

As parenchyma provides about 90% of the lung's volume and varies little if at all from one region of the lung to another, it is readily possible to acquire random fields of view of parenchyma from which quantitative data may be obtained. Our procedure was to place the microscope objective at random over the lung specimen exposed at the surface of the epoxy embedment, collect a depth series of images, return to the initial starting depth, move two field widths in the positive x direction, and repeat the process. Twenty-five depth series per piece of lung (for a total of 100 fields of view

per animal) were obtained in this way. (If the perimeter of the lung section was encountered, the objective was moved two field widths in the positive *y* direction, and the stepping was continued in the negative *x* direction.) At each location, if the profile of a conducting airway was in the volume to be recorded by the depth series, the field of view was skipped, and another step was made, until a volume was found that did not contain an airway. Each volume was recorded by obtaining 25 optical sections separated by 0.3 μm along the *z* axis. The real-world dimensions of a volume, therefore, were 61.6 μm × 61.6 μm × 7.5 μm in *x, y,* and *z,* respectively. More than 75,000 micrographs of the parenchyma region were recorded to obtain the necessary quantitative information.

The number of fibers in each volume was counted by a human operator who was able to move up and down through the depth series of images while looking for the characteristic bright points or lines that indicated a reflective or refractile particle or fiber. The person counting fibers did not know which experimental group the images were drawn from; that is, the counting was done under "single blind" conditions. These counts provided data with units of number of fibers per volume of parenchyma in cubic micrometers. Knowing the volume represented by each depth series and the volume of parenchyma (including airspaces) in the animal's entire lungs, as fixed, the fiber load in the lung's parenchyma could be calculated.

Whenever a fiber was detected, the anatomic compartment in which it occurred was also noted. In instances where free ends of the fiber were observed, fiber length was recorded using three-dimensional measurement techniques. Fibers in parenchyma were classified as occurring: in alveoli, alveolar ducts, or respiratory bronchioles, in contact with the surface of tissue; in ducts or alveoli, but not in contact with tissue in the recorded volume; and wholly or partly inside alveolar macrophages. Fibers observed in other parenchymal contexts such as interstitium or broncho-associated lymphoid tissue (BALT) were noted in the "other" category. These counts made it possible to estimate the fraction of fiber present in the different categories.

Sampling Strategy for Airways

Airways occupy only 10% of total inflated lung volume and exist as a treelike structure that is relatively coarse compared to parenchymal struc-

TABLE 2. Number and size distribution of the fibers in the chrysotile exposure aerosol

Exposure group	Gravimetric concentration (mg/m^3)	Number of fibers evaluated	Number of total fibers/cm^3	WHO fibers/cm^3	Percent WHO fibers	Number of fibers ⩾20 μm/cm^3	Percent of WHO fibers ⩾20 μm/cm^3
Air control	0	2	0.3	0	0	0	0
Canadian chrysotile	4.32 (0.36)	2482	14,805	1849	13	200	1

tures. Therefore, a field of view positioned at random on a lung sample has a rather low probability of containing any airway wall profile. Instead, it was efficient and valid to proceed along a randomly positioned line on the lung sample's surface and record volumes whenever the line encountered an airway whose local axis was nearly enough parallel to the sample surface's normal that the tissue layers in the airway wall were readily discerned.

Ten depth series (dimensions identical to parenchymal depth series) were recorded from each of 4 samples per animal, and these stacks held, on average, 75 μm of airway wall profile each. More than 30,000 micrographs of the airways were recorded and quantified from the airway category.

The average airway diameter in these lungs is estimated at 300 μm, and airway volume, as noted, is ~10% of lung volume. These numbers allow a further estimate of the length of an equivalent cylinder and its wall area, which is an estimate of the total airway wall area in the lungs.

Having measured the number of fibers per area of airway wall, the total fiber burden in the airway compartment was estimated.

Inflammatory Cells

Inflammatory cells were identified by morphologic recognition in serial section image data. The nuclear morphology of the cells and that of the surrounding pulmonary tissue are distinguished due to variations in fluorescent staining. Mononuclear cells, such as alveolar macrophages, were easily distinguished from neutrophils, which exhibit polymorphonuclear profiles.

RESULTS

Inhalation Biopersistence

The EC Inhalation Biopersistence Protocol specifies that the exposure atmosphere to which the animals are exposed should have at least 100 fibers/cm^3 longer than 20 μm. In this study, the number of fibers longer than 20 μm in the exposure atmosphere was purposely increased to a mean of 200 fibers/cm^3 longer than 20 μm, in order to maximize any potential effect of these long fibers on clearance from the lung. The number, concentration, and size distribution of the air control and chrysotile exposure group are shown in Table 2.

Diameter range (μm)	Length range (μm)	GMD (μm) (SD)	GML (μm) (SD)	Mean diameter (μm), SD	Mean length (μm), SD	Length-weighted arthm. diameter (μm)	Length-weighted geom. diameter (μm)	Aspect ratio
0.05–0.13	1.5–3.5	0.08	2.29	0.09	2.5	0.07	0.07	40.8
0.02–1	0.5–110	0.12	2.42	0.14	3.32	0.16	0.12	36.1

As illustrated in Figure 4, all of the longer fibers ($L > 20$ μm) in the exposure atmosphere were less than 1 μm in diameter (99.6% less than 0.8 μm) and thus potentially respirable. Figure 5 shows the bivariate length and diameter distribution of the fibers recovered from the lung at 1 day following cessation of exposure. The mean concentrations and dimensions of the fibers recovered from the lungs at each time point are presented in Table 3.

Photomicrographs of the original bulk sample and an aerosol sample taken using scanning electron microscopy (SEM) are shown in Figures 6 and 7. SEM was used for these micrographs in order to provide a visual overview of the fiber size distribution. As described earlier, transmission electron microscopy (TEM) was used for all quantification of fiber size.

Fiber Clearance

The fibers longer than 20 μm that deposit in the lung rapidly "disappear" from the lung as shown in Figure 8, with a clearance half-time of the fibers longer than 20 μm of 16 days. The clearance half-times (Table 4) were deter-

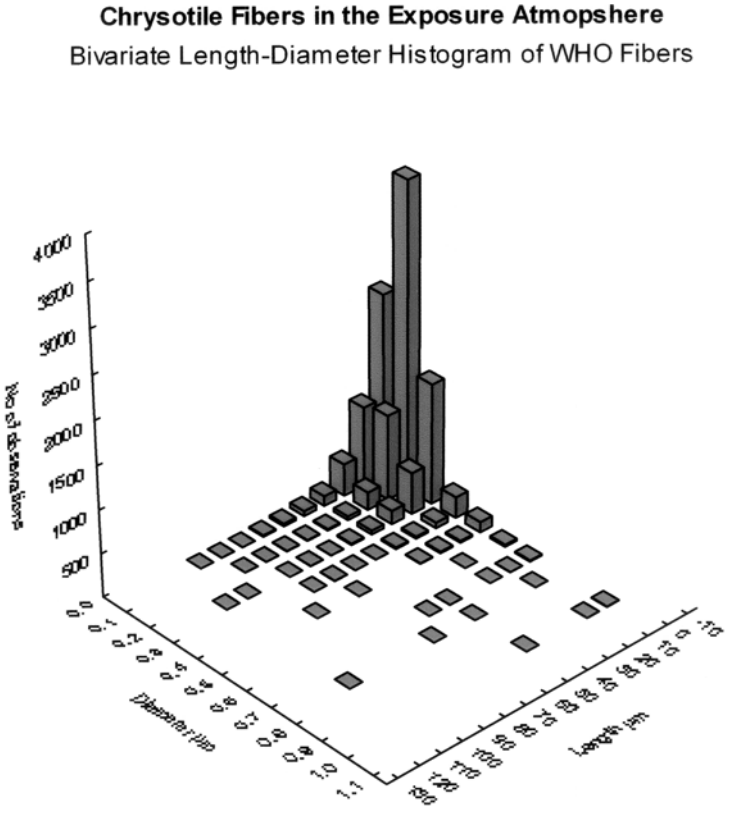

FIGURE 4. Bivariate length and diameter histogram of the chrysotile WHO fibers in the exposure atmosphere.

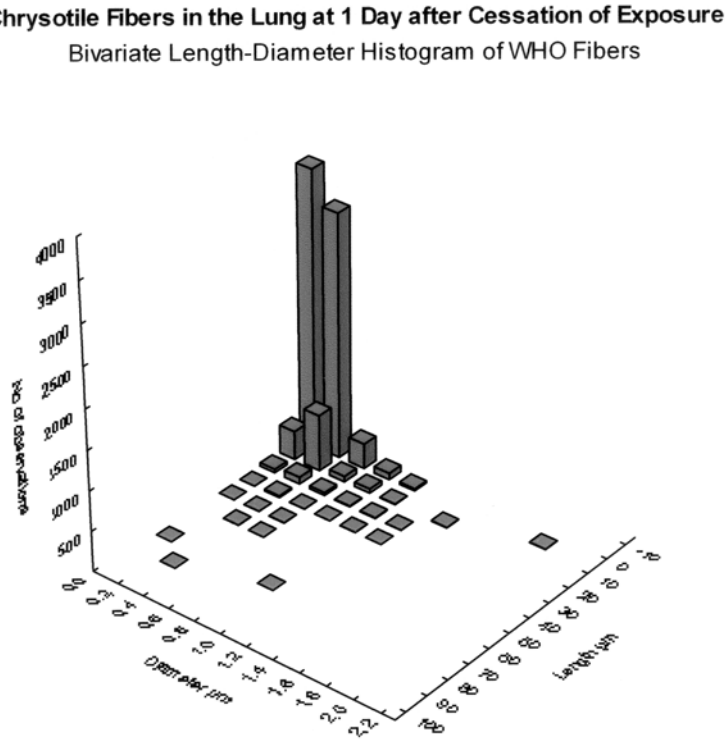

FIGURE 5. Bivariate length and diameter histogram of the chrysotile WHO fibers recovered from the lung at 1 day following cessation of exposure.

mined using the procedures specified in the EC Inhalation Biopersistence protocol (Bernstein & Riego-Sintes, 1999). The clearance curve was fitted to the data using nonlinear regression techniques with a double exponential (StatSoft, Inc., 2003).

At 30 days postexposure, a mean of 1.9 fibers was measured microscopically on the filter of the aliquot taken from the digestion of the whole lung. As shown in Table 3, this corresponds when extrapolated to the whole lung to 20,000 fibers $L > 20$ μm/lung at 30 days. After similar exposure of the insoluble amphibole fiber amosite, there would be approximately 1,000,000 fibers $L > 20$ μm/lung remaining at 30 days (extrapolated from Hesterberg et al., 1998).

As seen in Table 5, the fibers 5 to 20 μm in length also clear rapidly from the lung although more slowly than the fibers $L > 20$ μm. The clearance curves for the 5–20 μm fibers and the objects <5 μm were best fit using a single exponential also fitted to the data using nonlinear regression techniques (StatSoft, Inc., 2003). While the objects with lengths <5 μm have the slowest clearance half-times, this may be strongly influenced by the breaking apart of the longer fibers, which serve as a replenishing source for the shorter fibers. The clearance half-time of the fibers <5 mm is, however, within the

TABLE 3. Summary data of the mean lung burden results as determined by transmission electron microscopy (fiber concentrations: means ± SD)

	Sacrifice time point (time since cessation of last exposure)						
Parameter	1 day	2 days	7 days	2 wk	1 mo	3 mo	12 mo
Number of fibers evaluated	328.7 ± 12.1	320.9 ± 10.8	319.6 ± 7.8	314.0 ± 2.8	308.3 ± 2.6	226.1 ± 21.3	
Number of total fibers per lung lobes (million)	95.68 ± 13.6	92.72 ± 21.2	93.94 ± 19.6	71.38 ± 3.7	56.76 ± 5.4	41.20 ± 2.9	
Number WHO fibers per lung lobes (million)	11.0 ± 3.3	9.7 ± 4.2	12.1 ± 2.5	8.2 ± 1.1	5.6 ± 1.3	1.4 ± 0.2	
Number WHO fibers of total fibers (%)	11.48	10.14	12.92	11.52	9.86	3.42	
Number of fibers $L > 20$ µm per lung lobes (million)	0.4 ± 0.2	0.3 ± 0.1	0.2 ± 0.09	0.1 ± 0.03	0.1 ± 0.03	0.02 ± 0.01	
Fibers $L > 20$ µm of total fibers (%)	0.36	0.28	0.24	0.18	0.14	0.06	
Number of fibers L 5–20 µm per lung lobes (million)	10.7 ± 3.2	9.4 ± 4.1	11.9 ± 2.5	8.1 ± 1.1	5.6 ± 1.3	1.4 ± 0.2	
Fibers L 5–20 µm of total fibers (%)	11.12	9.88	12.68	11.32	9.76	3.36	
Number of fibers $L \leq 5$ µm per lung lobes (million)	84.7 ± 12	83.0 ± 17.6	81.8 ± 17.2	63.1 ± 2.8	51.1 ± 4.8	39.8 ± 2.7	
Fibers $L \leq 5$ µm of total fibers (%)	88.52	89.86	87.08	88.48	90.14	96.58	
Diameter range (µm)	0.02–1.3	0.02–1.1	0.03–1	0.03–0.09	0.03–0.09	0.02–0.8	
Length range (µm)	0.07–62	0.9–43	0.8–46	0.8–42	0.8–40	0.7–41	
Mean diameter (µm)	0.17	0.15	0.16	0.14	0.11	0.10	
SD	0.17	0.17	0.12	0.11	0.12	0.20	
Mean length (µm)	2.93	2.70	3.11	2.87	2.73	2.33	
SD	8.84	7.34	7.22	6.37	5.79	10.77	
GMD (µm)	0.14	0.12	0.13	0.11	0.09	0.07	
SD	2.11	2.25	1.99	1.98	2.23	2.51	
GML (µm)	2.29	2.17	2.51	2.33	2.23	1.85	
SD	3.44	3.30	2.99	2.99	2.97	3.59	
Length-weighted arthm. diameter (µm)	0.21	0.19	0.18	0.16	0.14	0.11	
Length-weighted geom. diameter (µm)	0.17	0.15	0.15	0.13	0.11	0.09	
Mode diameter (µm)	0.16	0.10	0.12	0.11	0.06	0.05	
Mode length (µm)	1.62	1.46	2.44	1.90	1.86	1.84	
Median diameter (µm)	0.16	0.14	0.15	0.11	0.09	0.07	
Median length (µm)	2.14	1.94	2.40	2.16	2.16	1.82	
Aspect ratio mean	22.15	25.06	26.88	26.86	30.65	31.84	
Number of particles evaluated	0.2	0	0	0	0	0.2	
Mean number of particles per lung lobes (million)	0.002	0	0	0	0	0.002	
≤1 µm particles per lung lobes (million)	0	0	0	0	0	0.002	
>1 µm–3 µm particles per lung lobes (million)	0	0	0	0	0	0	
>3 µm particles per lung lobes (million)	0.002	0	0	0	0	0	

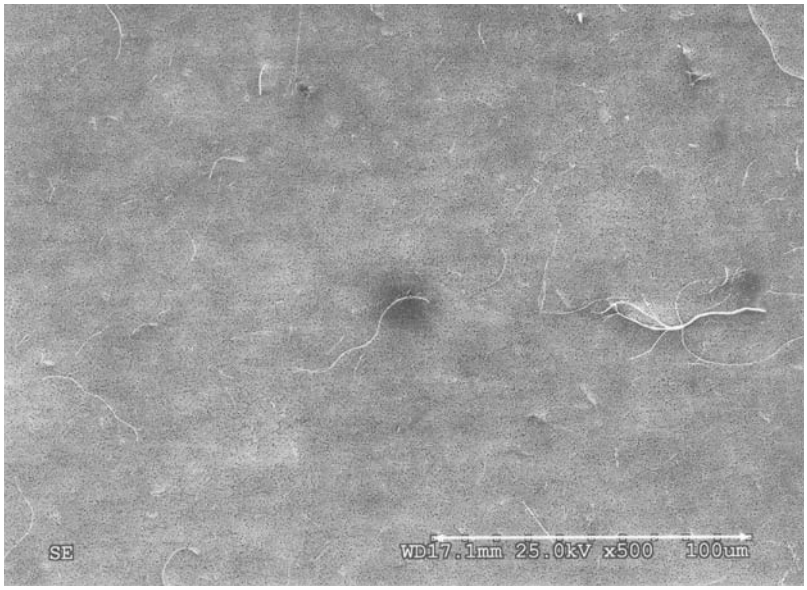

FIGURE 6. Photomicrographs of the original bulk chrysotile sample taken using scanning electron microscopy (SEM). SEM was used for these micrographs in order to provide a visual overview of the fiber size distribution. As described earlier, transmission electron microscopy (TEM) was used for all quantification of fiber size.

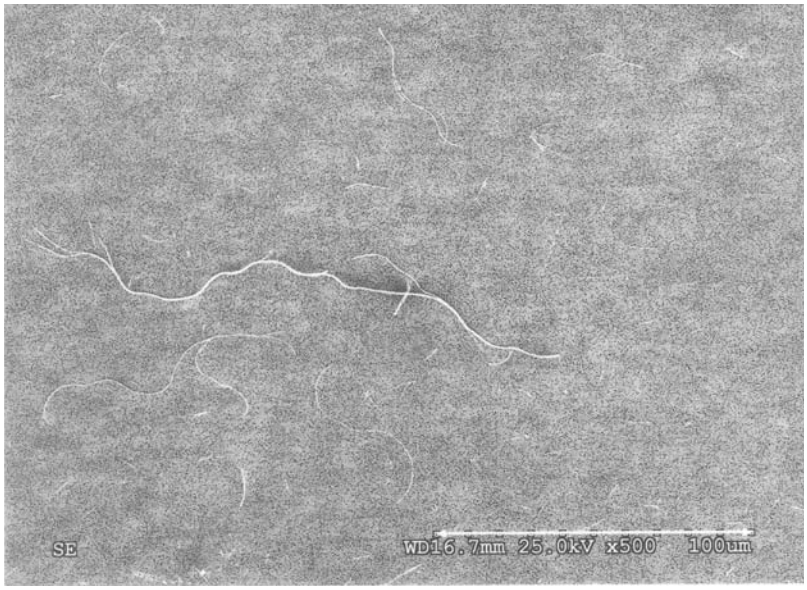

FIGURE 7. Photomicrographs of chrysotile fibers from an aerosol sample taken using scanning electron microscopy (SEM). SEM was used for these micrographs in order to provide a visual overview of the fiber size distribution. As described earlier, transmission electron microscopy (TEM) was used for all quantification of fiber size.

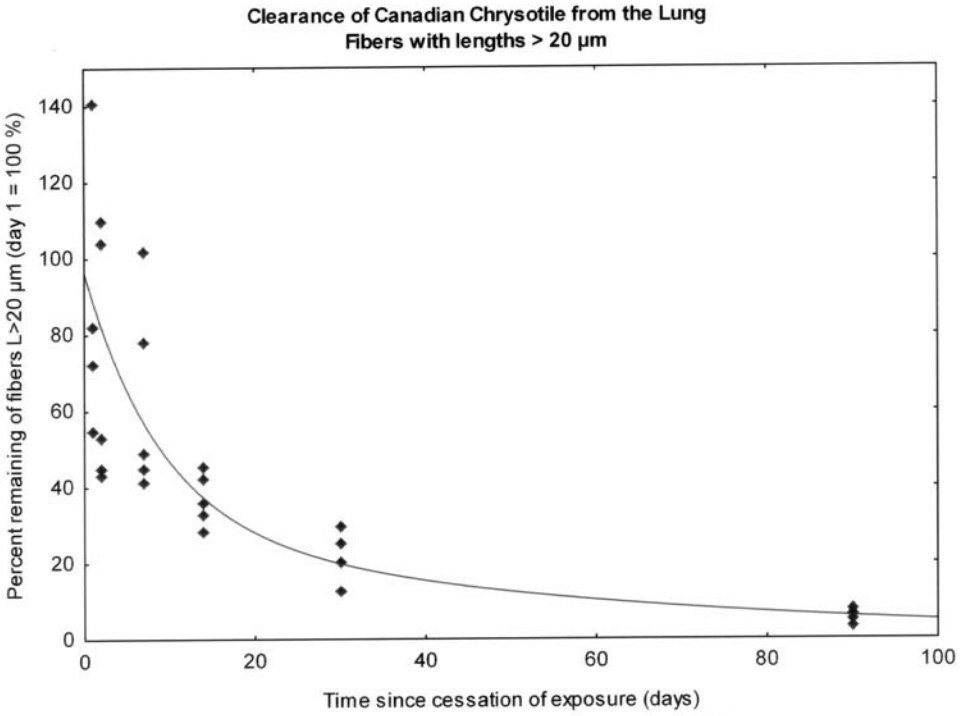

FIGURE 8. Graph showing the clearance of the Canadian chrysotile fibers longer than 20 µm from the lung following cessation of the 5-day exposure period. The diamonds indicate the percent remaining of the individual lungs. The solid line is the clearance curve fitted to the data using nonlinear regression techniques with a double exponential (StatSoft, Inc., 2003). The regression coefficients are presented in Table 4. (Note that five lungs were analyzed at each time point; however, in the figure some points are superimposed on each other.)

range of clearance for insoluble nuisance dusts (Muhle et al., 1987; Stoeber et al., 1970).

Confocal Microscopic Analysis

The classic biopersistence study as defined by the EC protocols involves the digestion of the entire rat lung for the determination of the fiber number

TABLE 4. Double-exponential fit to the data, fibers $L > 20$ µm, $R = .80119$, variance explained 64.190%

	a1	a2	T1	T2	$WT_{1/2}$
Estimate	65.96	30.38	6.16	38.04	16.22
SE	19.78	19.04	3.21	15.56	2.67
$t(26)$	3.33416	1.59552	1.918053	2.44419	6.06857
p Level	.00258	.12268	.066150	.02161	.00000

$WT_{1/2}$: weighted clearance half-time (Bernstein & Riego-Sintes, 1999).

TABLE 5. Clearance half-times of Canadian chrysotile by length fraction

Fiber length	Clearance half-time $T_{1/2}$
>20 μm	$WT_{1/2}$ = 16 days
5–20 μm	$T_{1/2}$ = 29.4 days
<5 μm	$T_{1/2}$ = 107 days

$WT_{1/2}$: weighted clearance half-time (Bernstein & Riego-Sintes, 1999).

and size distribution at each time point. The TEM analysis of ashed samples provides a measure of only the total number and size of fibers. It cannot detect where the fibers are located within the lung.

In order to determine the disposition of those fibers remaining in the lung, confocal microscopic analysis was performed on lobes of lungs embedded in plastic. A lens such as the one on a microscope that is closest to the sample to be examined (the objective lens) brings light to a focus at a certain, fixed distance. If the lens is well designed and constructed, there will be a plane where objects will be in focus. To use a conventional microscope effectively, it is necessary to cut a very thin slice of material to avoid tissue above and below the plane of focus from degrading the quality of the final image. The confocal microscope goes beyond the conventional microscope in this regard, because it excludes out-of-focus light using a light-limiting aperture to form a sharp, high-quality image even if there is material present that is not at the plane of focus. This means that specimens do not have to be thin sectioned before they can be examined. Instead, it is possible to obtain an image of the material at the plane of focus even if that plane lies tens of micrometers deep within the specimen.

Microscopical Appearance of the Chrysotile Fibers Retained in Lung

The limit of detection of the confocal method used to quantify the disposition of the chrysotile fibers in the lung was approximately 150 nm point-to-point resolution. Since most fibers were orientated to present various oblique profiles in longitudinal orientation, most fibrils greater than 150 nm in diameter were detected. This provided an accurate account of all fibers longer than 20 μm in the lung on day 1 as shown in Figure 9, as all such fibers observed by TEM were thicker than 0.15 μm. Shorter fibers with diameters greater than 0.15 μm were present in considerably larger number than thinner fibers (diameter < 0.15 μm) so as to provide an excellent account of the disposition of these length fibers as well. Similar results were seen throughout the study with the results obtained from TEM from 3 months shown in Figure 10. It is interesting to note that the shorter fibers (especially below 5 μm in length) with diameter >0.15 μm are decreasing in number, which suggests that the remaining chrysotile continues to be removed by macrophages and/or dissolves in the lung.

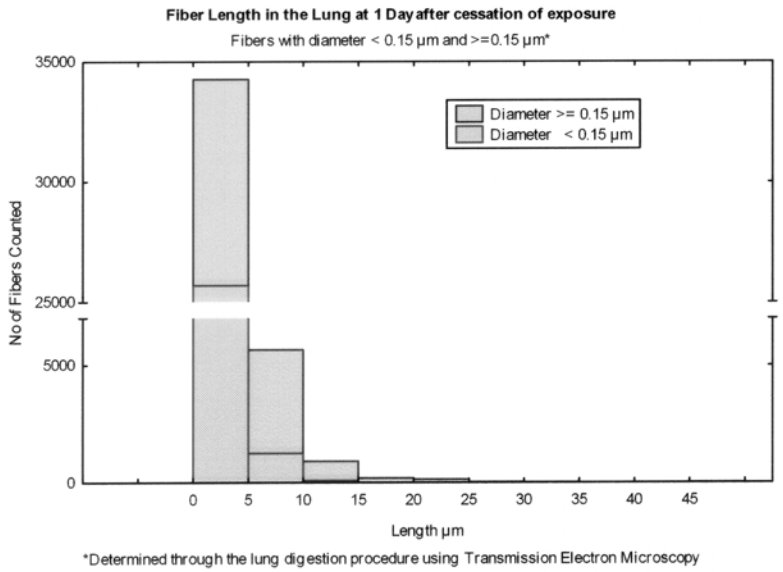

FIGURE 9. Length histogram (TEM) of fibers recovered from lungs at 1 day following cessation of exposure for those fibers that were <0.15 µm in diameter and >0.15 µm in diameter. Confocal microscopy measurements, which have a detection limit of 150 nm thus provide an accurate account of all fibers longer than 20 µm in the lung, as all such fibers observed by TEM were thicker than 0.15 µm. Shorter fibers with diameters greater than 0.15 µm were present in considerably larger number than thinner fibers (diameter <0.15 µm) and provide an excellent account of the disposition of these length fibers as well.

Parenchymal Fiber Load At all exposure time points, the parenchyma contained 99% of the total fiber load.

Sixty-eight percent of the fibers and particles seen at 1 day after cessation of exposure were found within alveolar macrophages, with the remainder occurring on epithelia of alveoli, alveolar ducts, and terminal bronchioles. This represents a substantial clearance of fibrils from the respiratory region at this time point. Similar observations were made at 2 days, 7 days, and 14 days after exposure.

At 1 mo after cessation of exposure, less than one-half (42%) of the fibers were detected inside alveolar macrophages, a decrease from that found at earlier exposure time points (68%, 60%, 69%, and 64% at 1, 2, 7, and 14 days, respectively). The balance of fibers observed at the 1-mo postexposure time point was located on the airway epithelia surfaces. It is important to note that compared to the 1-day postexposure group, 92% of all fibers have been cleared from the lungs by 1 mo postexposure.

Airway Fiber Load Taking the airway fiber load in the 1-day postexposure group as 100%, the fiber loads in the 2-day, 7-day, 14-day, and 1-mo postexposure groups are respectively 69%, 45%, 54%, and 29%.

Partitioning of Fiber Load Within Airway Compartment In the airways of the 1-day postexposure animals, 31% of the particles were found in airway

macrophages, in contrast to that seen in the 14-day postexposure animals, where 58% were found in airway macrophages. With the exception of the 14-day postexposure group, higher numbers of fibrils were observed on the surface of airway epithelia. The fibers on the airway epithelium and free in the airway lumens accounted for 62% of the fiber load, about 2 times that of the fiber load carried by airway macrophages. This indicates a steady, long-term clearance pathway by ciliated epithelium within conducting airways, supplemented by airway macrophage clearance.

Lung Fiber Lengths in Parenchyma and Airways

Fiber length within parenchyma, by time point The mean fiber length was between 5.5 and 7.4 μm. The number of fibers longer than 20 μm rapidly decreased by a factor of 5 from 1 day postexposure to 2 days post-exposure. No fibers greater than 20 μm were observed in parenchyma at 1 mo postexposure. These data strongly support that fibers, upon contact with lung surfaces and cells, rapidly disintegrate into shorter fibrils.

Fiber length within airways, by time point Fiber lengths in the airways were, on average, longer than those seen in the parenchymal region. In general, average fiber lengths were in the range of 7 to 9 μm. Very few fibers longer than 20 μm were observed in any animal, and by 1 mo after cessation of exposure, no fibers greater than 20 μm were observed in randomly collected image data.

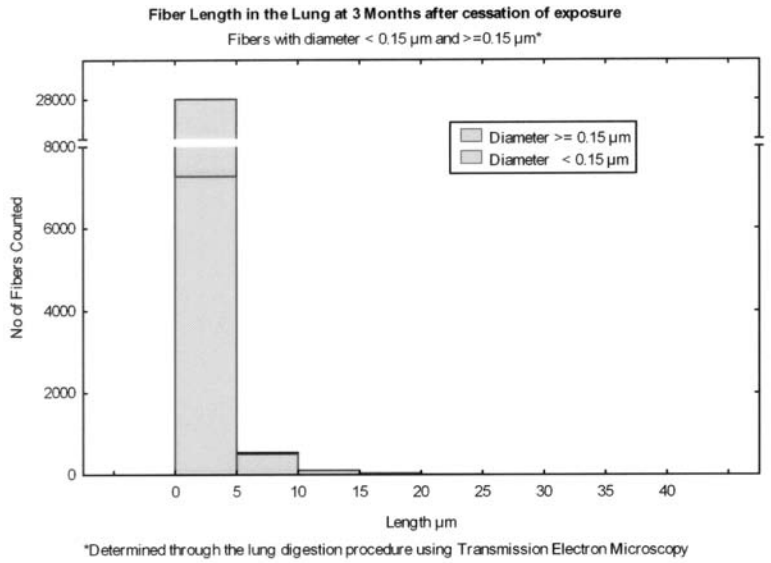

FIGURE 10. Length histogram (TEM) of fibers recovered from lungs at 3 mo following cessation of exposure for those fibers that were <0.15 μm in diameter and >0.15 μm in diameter. This confocal microscopy measurement, which has a detection limit of 150 nm, thus provides an accurate account of all fibers longer than 20 μm in the lung, as all such fibers observed by TEM were thicker than 0.15 μm. Shorter fibers with diameters greater than 0.15 μm were present in considerably larger number than thinner fibers (diameter <0.15 μm) and provide an excellent account of the disposition of these length fibers as well.

Inflammatory Cells Neutrophils were not observed free in alveolar spaces in any of the data volumes collected. Neutrophil-mediated inflammatory response did not occur in the presence of chrysotile fibers at the time points examined to date.

Time Course—Confocal Imaging The disposition of the chrysotile fibers in the lung from 1 day through 30 days after cessation of exposure is shown in the confocal micrographs, which were image processed to identify through color coding of the profiles of the Canadian chrysotile fibrils in context with lung tissue.

At 1 day after cessation of exposure, the chrysotile fibers appeared to have been well distributed throughout the lung in both airway and parenchyma. As shown in Figure 11, fibers appeared as separate, fine fibrils, occasionally unwound at one end and were not found clumped together. Fibers were found on the surface of a ciliated airway (Figure 11a), in the alveoli (Figure 11b), phagocytosed by alveolar macrophages (Figure 11c), and the shorter fibers were found to be transported to the distal pulmonary lymphatics (Figure 11d).

By 1 mo after cessation of exposure, Figure 12 shows four regions similar to those shown at 1 day (Figure 11). These are the airway wall (Figure 12a), the alveoli (Figure 12b), fibers in the alveolar macrophages (Figure 12c), and the distal pulmonary lymphatics (Figure 12d). While some fibers are found in each of these regions, it is notable that number and length of fibers observed are greatly reduced.

The numbers of fibers quantified using confocal examination are shown as a function of time for the parenchyma (Figure 13) and for the airway (Figure 14) regions of the lung. The parenchyma and the airway were each subdivided into four compartments as defined next. In addition, the inflammatory cells present were also identified.

Definitions:

Parenchyma

1. *Touching alveolar, ductal epithelium:* Those fibrils observed in serial section series to have at least one end, or portions in direct contact with alveolar, of alveolar duct epithelium.
2. *In alveolar macrophage:* Fibrils observed in serial section series to have been completely internalized by phagocytic engulfment, or portions along the length in direct contact with alveolar macrophage. This also includes fibrils with at least one end in contact with alveolar macrophages.
3. *Seen in alveolar, ductal airspace:* Those fibrils observed in serial sections to have no direct contact with alveolar, of alveolar duct epithelium.
4. *Another location in parenchyma:* Those fibrils observed in serial section series to have at least one end, or portions in direct contact with other structures in parenchyma, such as subepithelial cells, interstitial spaces, lymphatic ducts, or indeterminate structures in the alveolar region.

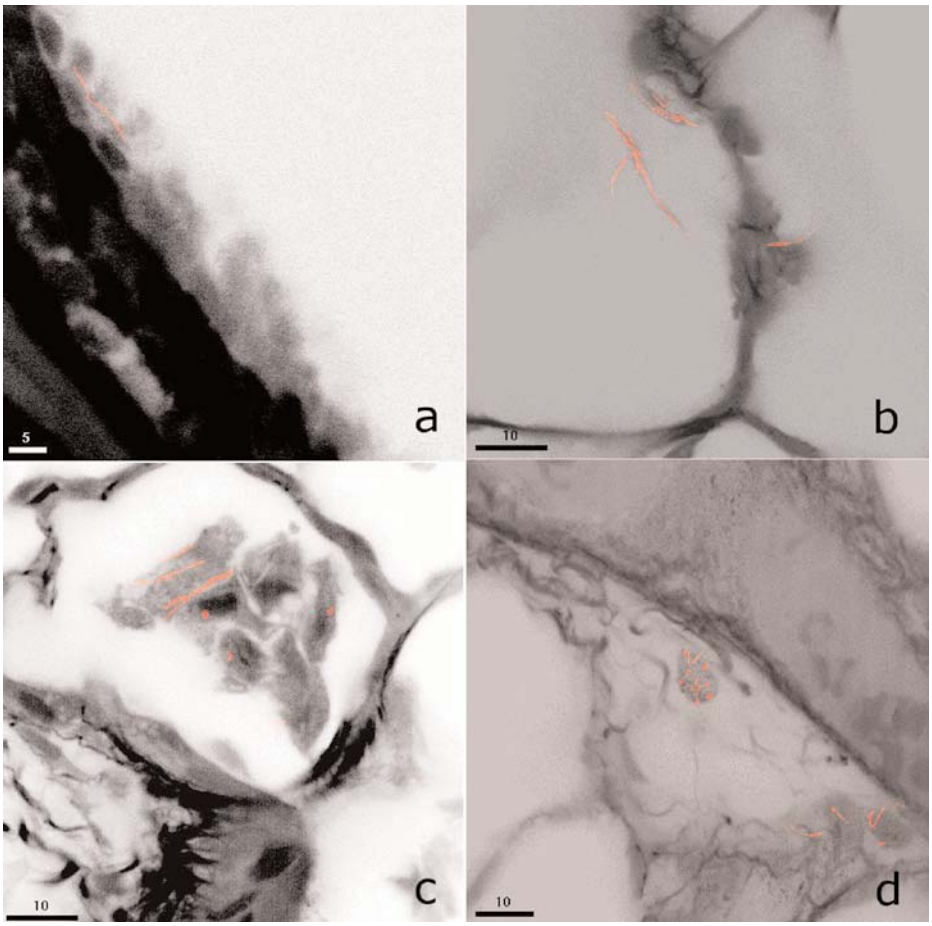

FIGURE 11. Confocal micrographs recorded from 1-day postexposure group. All images were digitally processed from original optical sections, approximately 0.5 μm thick, recorded from undisturbed regions of the lung. Pulmonary tissue appears as a gray-scale composite with profiles of test article (red). Fibers were found on the surface of ciliated airways. (A) Cross section of a large airway with a thin fibril resting on ciliated epithelial cells. Scale bar is 5 μm. Fibers were observed in the alveoli. (B) Typical field of view in the parenchymal region reveals numerous fibrils next to an alveolar wall and a few fibrils appearing free in the alveolar space. Scale bar is 10 μm. Fibers were frequently observed to have been phagocytosed by alveolar macrophages. (C) Fiber clearance by alveolar macrophages. Numerous alveolar macrophages appear to surround fibrils in the alveolar space. These cells are known to carry foreign material from the gas exchange region to the airways, ultimately to be swept up to the trachea and cleared from the pulmonary compartment altogether. Scale bar is 10 μm. The shorter fibers were found to be transported to the distal pulmonary lymphatics. (D) Distal pulmonary lymphatic duct containing short chrysotile fibrils, as well as a cell containing numerous chrysotile profiles. It is clear the pulmonary lymphatics are a clearance pathway for material deposited via inhalation exposure. Scale bar is 10 μm.

Airways

1. *On surface of or intercalated within ciliated epithelium of conducting airway:* Those fibrils observed in serial section series to have at least one end, or portions in direct contact with epithelium of conducting airways, or observed to be in contact with cells immediately subjacent to the epithelium of conducting airways.

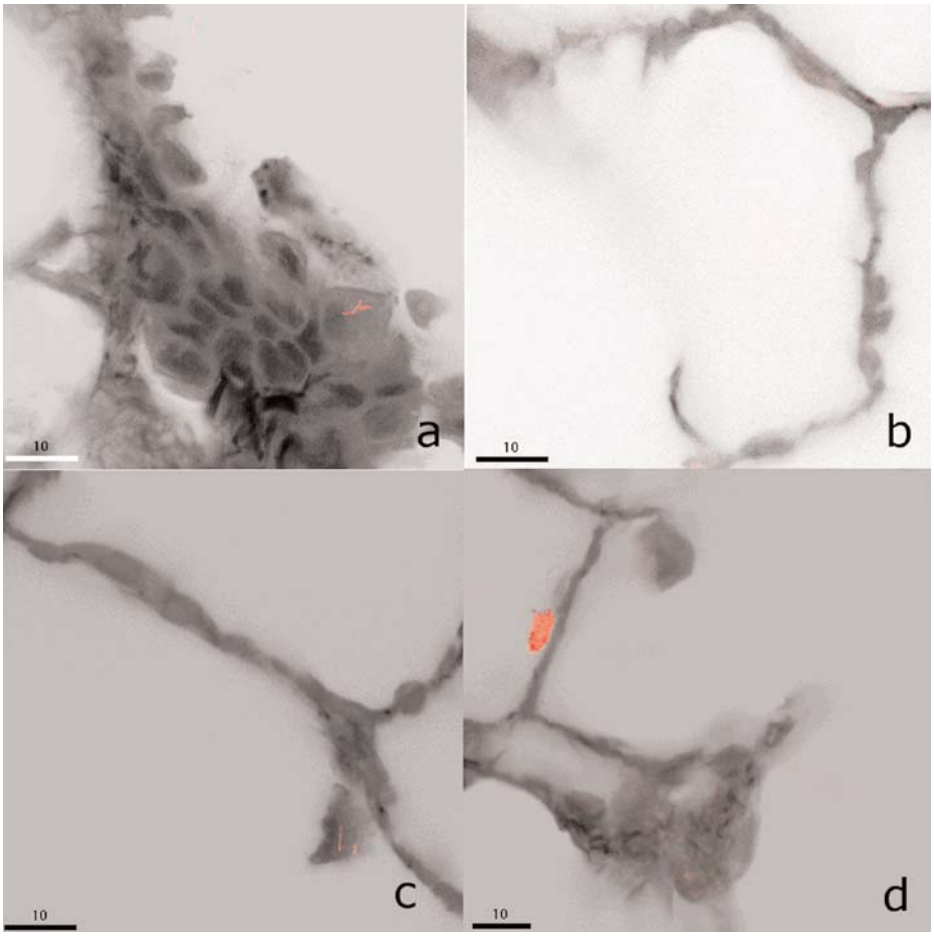

FIGURE 12. Confocal micrographs recorded from the 1-mo postexposure group. All images were digitally processed from original optical sections, approximately 0.5 μm thick, recorded from undisturbed regions of the lung. Pulmonary tissue appears as a gray-scale composite with profiles of test article (red). At this time point, very few micrographs actually contain profiles of the test article. These particular images were selected to show the appearance of chrysotile, when present. Fibers were found on the surface of ciliated airways. (A) Cross section of a large ciliated airway near a bifurcation with a short, thin fibril inside a cell adjacent to the epithelium. Scale bar is 10 μm. Fibers were observed in the alveoli. (B) Typical field of view in the parenchymal region showing an alveolar wall, and alveolar space. Scale bar is 10 μm. Occasional fibers were observed phagocytosed by alveolar macrophages. (C) Fiber clearance by an alveolar macrophage. Scale bar is 10 μm. Very few fibrils were observed in alveolar interstitial spaces, including distal pulmonary lymphatics. (D) Distal pulmonary lymphatic duct (lower center of the image) devoid of any chrysotile fibrils. Calcified structures were occasionally found on the alveolar epithelium, but no adverse tissue response has been observed associated with these structures. Scale bar is 10 μm.

2. *Within airway macrophage:* Fibrils observed in serial section series to have been completely internalized by phagocytic engulfment, or portions along the length in direct contact with a macrophage in a conducting airway. This also includes fibrils with at least one end in contact with airway macrophages.

3. *In airway lumen; portion of fiber visualized not touching tissue:* Those fibrils observed in serial section series to have no direct contact with conducting airway epithelium.
4. *Another location in airway:* Those fibrils observed in serial section series to have at least one end, or portions in direct contact with other structures in conducting airway structures, such as interstitial spaces, broncho-associated lymphoid tissue,lymphatic ducts, or other indeterminate structures.
5. *Identification of inflammatory cells:* Inflammatory cells were identified by examination in serial section image data the nuclear morphology of cells and surrounding pulmonary tissue. Mononuclear cells, such as alveolar macrophages, were easily distinguished from neutrophils, which exhibit polymorphonuclear profiles.

For both the parenchyma and airway regions, from 1 day to 30 days after cessation of exposure there is a marked reduction in the number of fibers observed in all compartments. As mentioned already, the large majority of fibers are found in the parenchyma with most of those found in the alveolar macrophages (Figure 11). By 1 mo postexposure, fibers were no longer observed in the interstitium.

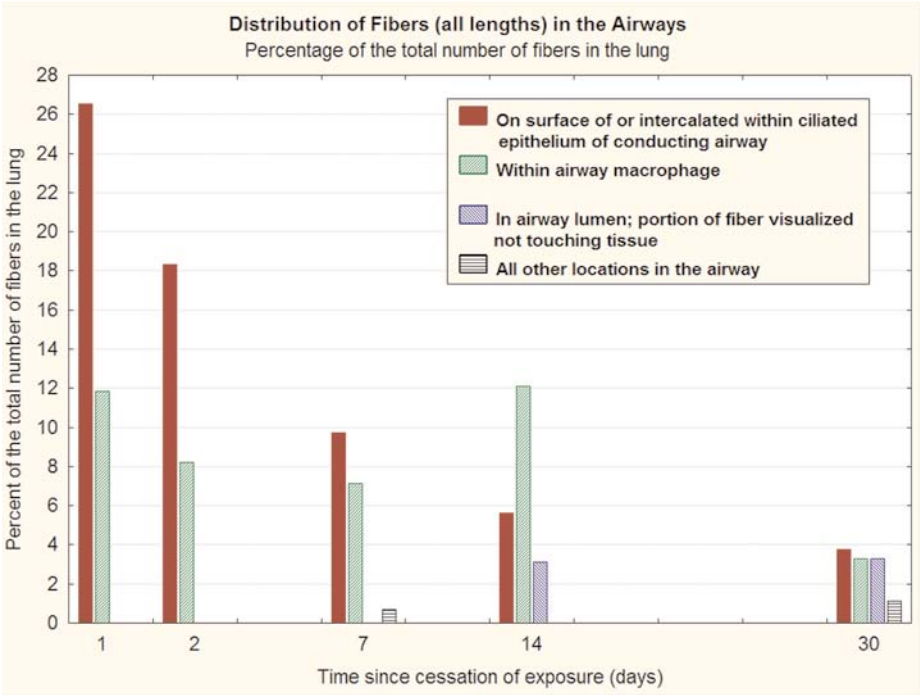

FIGURE 13. The numbers of fibers quantified using confocal examination are shown as a function of time for the parenchyma region of the lung. As defined in the text, the parenchyma was subdivided into the following four compartments: fibers touching alveolar, ductal epithelium; in alveolar macrophage; seen in alveolar, ductal airspace; and another location in parenchyma.

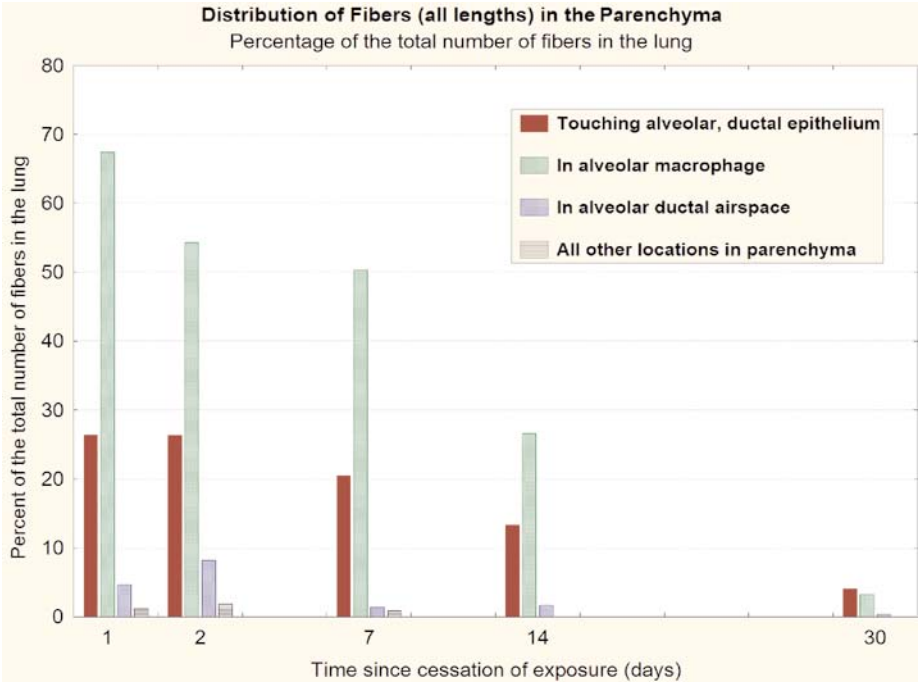

FIGURE 14. The numbers of fibers quantified using confocal examination are shown as a function of time for the airway region of the lung. As defined in the text, the airway was subdivided into the following four compartments: fibers on surface of or intercalated within ciliated epithelium of conducting airway; within airway macrophage; in airway lumen—portion of fiber visualized not touching tissue; and another location in airway.

While these confocal images provide quantification of where the chrysotile fibers are in the lung, they do not show the surrounding lung surfactant which is very important in mediating dissolution in the lung. Nearly all the fibers observed are within the surfactant layer and therefore more readily subject to dissolution with the biodegradation of chrysotile being diffusion-dependent (Atkinson, 1973). In addition, Etherington et al. (1981) has shown that macrophages can generate very low pH at the surface of the macrophage membrane and, in particular, within the macrophage phagolysosome that surrounds the particles, pH values as low as 3.5 are encountered. Chrysotile is most soluble at such acid pH. When in contact with dilute acids or even aqueous media at pH < 10, magnesium has been shown to readily dissociate from the fiber's surface (Hargreaves & Taylor, 1946; Atkinson, 1973; Nagy & Bates, 1952) resulting in a leached fiber (Atkinson, 1973). The results of our study are consistent with these proposed mechanisms leading to the breakup of longer chrysotile fibers into shorter pieces.

DISCUSSION

Fiber Structural Chemistry and Rapid Dissolution

In chrysotile, the magnesium hydroxide part of each layer is closest to the fiber surface and the silica tetrahedral is within the structure (see Figure 1). In water, the dissolution of chrysotile has been shown to be affected by the buffer capacity of the leach solution, with the amount of extractable Mg and SiO_2 increasing with increasing buffer strength (Smith, 1973). This reaction has been determined to be diffusion controlled through a layer of water near the mineral's surface.

In the lung, extensive work on modeling the dissolution of synthetic mineral fibers (SMF) using in vitro dissolution techniques and inhalation biopersistence has shown that the lung has a very large buffer capacity (Matson, 1994). These studies have shown that an equivalent in vitro flow rate of up to 1 ml/min is required to provide the same dissolution rate of SMF as that which occurs in the lung. In addition, chrysotile is more soluble at acid pH and thus may be affected by complete or even partial phagocytosis of fibers by macrophages.

With the chrysotile tested, it appears that as the magnesium dissolves, the fiber breaks apart into smaller pieces. Thus, while the rats were exposed to a very large number of long respirable fibers (200 fibers $L > 20$ μm/cm^3, GMD = 0.12 μm), it was observed that by day 6 of the study (1 day after cessation of exposure) already a large number of fibers had dissolved/disintegrated.

Dose Delivered and Comparative Clearance

To assess how much of the deposited dose had been cleared from the lung by the first time point of analysis (day 1 after cessation of exposure) and what the relative lung burdens are of chrysotile in comparison to an amphibole and a highly soluble fiber, we compared the data from this study to that from an inhalation biopersistence study of amosite asbestos and the soluble stonewool fiber MMVF 34 (Kamstrup et al., 1998). In the Hesterberg et al. (1998) study, the aerosol exposure concentrations were 150 fibers $L > 20$ μm/cm^3. The GMD of the WHO fibers was reported as 0.48 μm and 0.73 μm for amosite and MMVF 34, respectively (the GMD of the long fibers was not reported). As described earlier, the chrysotile exposure concentrations were 200 fibers $L > 20$ μm/cm^3 with GMD of these fibers of 0.12 μm and thus were also rat respirable.

To compare the two studies, we multiplied the lung burdens of the fibers $L > 20$ μm given by Hesterberg et al. (1998) by 2 to provide "calculated" equalized doses as the chrysotile exposure of long fibers in our study was twice that of the Hesterberg study. The numbers of fibers in the lung as a function of time since cessation of exposure is shown in Figure 13. If chrysotile was insoluble, on day 1 after cessation of exposure, approximately 5 ×

10^6 fibers with $L > 20$ μm would have been found in the lung as seen for amosite and MMVF 34. The chrysotile, however, is so soluble that only approximately 3×10^5 fibers $L > 20$ μm or 6% remain in the lung at 1 day after cessation of the 5-day exposure. The clearance of MMVF 34, which has a reported half-time of 6 days (Hesterberg et al., 1998), is seen to quickly diverge from that of amosite most of which remains in the rat for its lifetime. By 90 days, more than 1×10^6 long amosite fibers remain. In comparison, the long MMVF 34 and chrysotile fibers are reduced by approximately 100-fold. This result is interesting as MMVF 34 was tested in a chronic inhalation study at high exposure concentrations and produced neither fibrosis nor tumors (Kamstrup et al., 1998). As shown in the panel insert in Figure 15, at 90 days after cessation of exposure, using the extended counting procedures already described, only 1 to 2.5 fibers longer than 20 μm were observed on the filter from the digested lung for each animal; thus, the levels present are rapidly approaching the background level.

Comparison with Other Chrysotile Biopersistence Studies

This study provides the first application of the EC biopersistence protocol to chrysotile. Ilgren and Chatfield (1997, 1998a, 1998b) reviewed a number of studies that provided estimates of clearance of chrysotile based upon the silica content of the lung. These studies reported clearance half-times considerably longer than that found here. This analysis, however, did not differentiate clearance as a function of fiber length or compartment within the lung. As seen in our study, the long chrysotile fibers clear most rapidly while some of the shorter fibers accumulate in the lung and lymphatics. Nearly all of these previous studies involved exposure periods of from 3 to 12 mo and used a range of exposure concentrations from 2 to 10 mg/m^3. With an exposure concentration of 10 mg/m^3, the total fiber concentration was more than 1×10^6 fibers (Mast et al., 1995). The number of nonfibrous particles was not reported, although from the current study this could equal the number of fibers. With these very high exposure concentrations it is likely that rat-specific lung overload occurred, which would present a serious bias in any lung clearance measurements (Oberdorster, 1995a, 1995b, 2002). In addition, in these studies there was no reported investigation of the presence of other silicates in the aerosol and especially of amphibole fibers such as tremolite. Wagner et al. (1980) stated that "all materials contained impurities" in the chrysotile samples that he studied, although he did not identify these impurities.

Fibers Remaining

We have seen that chrysotile clears with a half-time of 16 days for fibers $L > 20$ μm. However, as stated, some long fibers are observed at 30 days. The question, of course, remains of whether these few remaining fibers are biologically relevant in producing a possible pathological response.

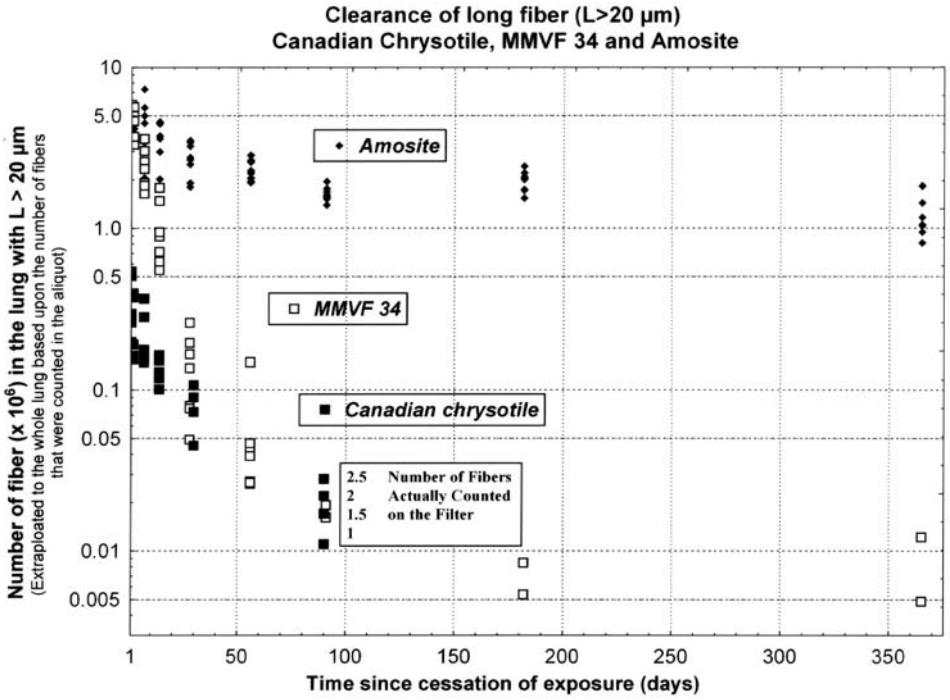

FIGURE 15. The number of fibers in the lung as a function of time since cessation of exposure is shown for Canadian chrysotile, MMVF 34 and amosite. If chrysotile was insoluble, on day 1 after cessation of exposure, approximately 5×10^6 fibers with $L > 20$ µm would have been found in the lung, as seen for amosite and MMVF 34. The chrysotile, however, is so soluble that only approximately 3×10^5 fibers $L > 20$ µm remain in the lung at 1 day after cessation of the 5-day exposure. The clearance of MMVF 34, which has a reported half-time of 6 days, is seen to quickly diverge from that of amosite, most of which remains in the rat for its lifetime. By 90 days, more than 1×10^6 long amosite fibers remain. In comparison, the long MMVF 34 and chrysotile fibers are reduced by approximately 100-fold. The panel insert shows that at 30 days after cessation of exposure, using the extended counting procedures described in the text, from 1 to 2.5 fibers longer than 20 µm were observed on the filter from the digested lung for each animal.

The question of the possible effect of shorter chrysotile fibers has been addressed by the chronic inhalation studies reported by Ilgren and Chatfield (1997, 1998a, 1998b). In these studies, rats were exposed for 7 h/day, 5 days/wk for 12 mo to a mean concentration of 7.8 mg/m^3 of Coalinga chrysotile. The Coalinga chrysotile was reported as being relatively short with the majority of fibers less than 5 µm in length. No fibrotic or tumorigenic response was observed following exposure to this fiber. Similar results were reported in another study with the Coalinga fiber by Muhle et al. (1987). In addition, the Coalinga fiber was tested in four chronic ip studies of up to 3 mg dose with tumor levels in the reported background range of up to 10% (Muhle et al., 1987; Pott et al., 1987; Rittinghausen et al.,

1992). These studies provide support that shorter chrysotile is not carcinogenic following both inhalation and ip exposure at relatively high concentrations. In addition, in a Report of the Expert Panel on Health Effects of Asbestos and Synthetic Vitreous Fibers: The Influence of Fiber Length, issued recently by the Agency for Toxic Substances and Disease Registry (ATSDR), it was stated that "Given findings from epidemiologic studies, laboratory animal studies, and in vitro genotoxicity studies, combined with the lung's ability to clear short fibers, the panelists agreed that there is a strong weight of evidence that asbestos and SVFs (synthetic vitreous fibers) shorter than 5 μm are unlikely to cause cancer in humans" (ATSDR, 2003).

CONCLUSION

Taken in context with the scientific literature to date, this report provides new robust data that clearly support the difference seen epidemiologically between chrysotile and amphibole asbestos.

REFERENCES

Agency for Toxic Substances and Disease Registry. 2003. *Report on the expert panel on health effects of asbestos and synthetic vitreous fibers: The influence of fiber length*. Prepared for: Agency for Toxic Substances and Disease Registry Division of Health Assessment and Consultation Atlanta, GA.

Atkinson, R. J. 1973. Chrysotile asbestos: Colloidal silica surfaces in acidified suspensions. *J. Colloid Interface Sci.* 42:624–628.

Bernstein, D. M., and Riego-Sintes, J. M. R. 1999. *Methods for the determination of the hazardous properties for human health of man made mineral fibers (MMMF)*. European Commission Joint Research Centre, Institute for Health and Consumer Protection, Unit: Toxicology and Chemical Substances, European Chemicals Bureau, EUR 18748 EN, April. http://ecb.ei.jrc.it/DOCUMENTS/Testing-Methods/mmmfweb.pdf

Bernstein, D. M., Mast, R., Anderson, R., Hesterberg, T. W., Musselman, R., Kamstrup, O., and Hadley, J. 1994. An experimental approach to the evaluation of the biopersistence of respirable synthetic fibers and minerals. *Environ. Health Perspect.* 102(suppl. 5):15–18.

Bernstein, D. M., Riego-Sintes, J. M., Ersboell, B. K., and Kunert, J. 2001. Biopersistence of synthetic mineral fibers as a predictor of chronic inhalation toxicity in rats. *Inhal. Toxicol.* 13(10):823–849.

Cannon, W. C., Blanton, E. F., and McDonald, K. E. 1983. The flow-past chamber: An improved nose-only exposure system for rodents. *Am. Ind. Hyg. Assoc. J.* 44(12):923–928.

Churg, A. 1994. Deposition and clearance of chrysotile asbestos. *Ann. Occup. Hyg.* 38(4):625–633.

Churg, A., and DePaoli, L. 1988. Clearance of chrysotile asbestos from human lung. *Exp. Lung Res.* 14:567–574.

Cossette, M., and Delvaux, P. 1979. Technical evaluation of chrysotile ore bodies. In *Short course in mineralogical techniques of asbestos determination,* ed. R. L. Ledoux, Vol. 4, pp. 79-110. Quebec: Mineralogical Association of Canada.

Etherington, D. J., Pugh, D., and Silver, I. A. 1981. Collagen degradation in an experimental inflammatory lesion: Studies on the role of the macrophage. *Acta Biol. Med. Ger.* 40(10–11):1625–1636.

Hargreaves, A., and Taylor, W. H. 1946. An x-ray examination of decomposition products of chrysotile (asbestos) and serpentine. *Min. Mag.* 27:204–216.

Hesterberg, T. W., Chase, G., Axten, C., Miiller, W. C., Musselman, R. P., Kamstrup, O., Hadley, J., Morscheidt, C., Bernstein, D. M., and Thevenaz, P. 1998. Biopersistence of synthetic vitreous fibers and amosite asbestos in the rat lung following inhalation. *Toxicol. Appl. Pharmacol.* 151(2): 262–275.

Hodgson, A. A. 1979. Chemistry and physics of asbestos. In *Asbestos: Properties, applications and hazards,* eds. L. Michaels and S. S. Chissick, pp. 80–81. New York: John Wiley & Sons.

Howard, J. K. 1984. Relative cancer risks from exposure to different asbestos fibre types. *N. Z. Med. J.* 97:646–649.

Ilgren, E., and Chatfield, E. 1997. Coalinga fibre—A short, amphibole-free chrysotile, Part 1: Evidence for a lack of fibrogenic activity. *Indoor Built Environ.* 6:264–276.

Ilgren, E., and Chatfield, E. 1998a. Coalinga fibre: A short, amphibole-free chrysotile, Part 3: Lack of biopersistence. *Indoor Built Environ.* 7:98–109.

Ilgren, E., and Chatfield, E. 1998b. Coalinga fibre—A short, amphibole-free chrysotile, Part 2: Evidence for lack of tumourigenic activity. *Indoor Built Environ.* 7:18–31.

Kamstrup, O., Davis, J. M., Ellehauge, A., and Guldberg, M. 1998. The biopersistence and pathogenicity of man-made vitreous fibres after short- and long-term inhalation. *Ann. Occup. Hyg.* 42(3):191–199.

Kiyohara, P. K. 1991. *Estudo da interface crisotila-cimento Portland em compósitos de fibro-cimento por métodos óptico-eletrônicos*. São Paulo: Tese de Doutorado, apres. EPUSP.

Mast, R. W., McConnell, E. E., Anderson, R., Chevalier, J., Kotin, P., Bernstein, D. M., Thevenaz, P., Glass, L. R., Miiller, W. C., and Hesterberg, T. W. 1995. Studies on the chronic toxicity (inhalation) of four types of refractory ceramic fiber in male Fischer 344 rats. *Inhal. Toxicol.* 7(4):425–467.

Matson, S. M. 1994. Glass fibres in simulated lung fluid: Dissolution behavior and analytical requirements. *Ann. Occup. Hyg.* 38:857–877.

McDonald, J. C. 1998. Mineral fibre persistence and carcinogenicity. *Ind. Health* 36(4):372–375.

McDonald, J. C., and McDonald, A. D. 1997. Chrysotile, tremolite and carcinogenicity. *Ann. Occup. Hyg.* 41(6):699–705.

McDonald, J. C., McDonald, A. D., and Hughes, J. M. 1999. Chrysotile, tremolite and fibrogenicity. *Ann. Occup. Hyg.* 43(7):439–442.

Morgan, A. 1994. The removal of fibres of chrysotile asbestos from lung. *Ann. Occup. Hyg.* 38(4):643–646.

Mossman, B. T., Bignon, J., Corn, M., Seaton, A., and Gee, J. B. L. 1990. Asbestos: Scientific developments and implications for public policy. *Science* 247:294–301.

Muhle, H., Pott, F., Bellmann, B., Takenaka, S., and Ziem, U. 1987. Inhalation and injection experiments in rats to test the carcinogenicity of MMMF. *Ann. Occup. Hyg.* 31(4B):755–764.

Muhle, H., Creutzenberg, O., Bellmann, B., Heinrich, U., and Mermelstein, R. 1990. Dust overloading of lungs: Investigations of various materials, species differences, and irreversibility of effects. *J. Aerosol Med.* 3(suppl. 1):111–128.

Nagy, B., and Bates, T. F. 1952. Stability of chrysotile asbestos. *Am. Mineral* 37:1055–1058.

Oberdorster, G. 1995a. Lung particle overload: Implications for occupational exposures to particles. *Regul. Toxicol. Pharmacol.* 21(1):123–135.

Oberdorster, G. 1995b. The NTP talc inhalation study: A critical appraisal focused on lung particle overload. *Regul. Toxicol. Pharmacol.* 21(2):233–241.

Oberdorster, G. 2002. Toxicokinetics and effects of fibrous and nonfibrous particles. *Inhal. Toxicol.* 14(1):29–56.

Pott, F., Ziem, U., Reiffer, F. J., Huth, F., Ernst, H., and Mohr, U. 1987. Carcinogenicity studies on fibres, metal compounds, and some other dusts in rats. *Exp. Pathol.* 32(3):129–152.

Rittinghausen, S., Ernst, H., Muhle, H., and Mohr, U. 1992. Atypical malignant mesotheliomas with osseous and cartilaginous differentiation after intraperitoneal injection of various types of mineral fibres in rats. *Exp. Toxicol. Pathol.* 44(1):55–58.

Rodelsperger, K., Woitowitz, H. J., Bruckel, B., Arhelger, R., Pohlabeln, H., and Jockel, K. H. 1999. Dose-response relationship between amphibole fiber lung burden and mesothelioma. *Cancer Detect. Prev.* 23(3):183–193.

Rogers, R. A., Antonini, J. M., Brismar, H., Lai, J., Hesterberg, T. W., Oldmixon, E. H., Thevenaz, P., and Brain, J. D. 1999. In situ microscopic analysis of asbestos and synthetic vitreous fibers retained in hamster lungs following inhalation. *Environ. Health Perspect.* 107(5):367–375.

Skinner, H. C. W., Ross, M., and Frondel, C., eds. 1988. *Asbestos and other fibrous minerals*, Figure 2.3, p. 31. Oxford University Press.

Smith, R. W. 1973. *Aqueous surface chemistry of asbestos minerals*. Cincinnati, OH: National Institute for Occupational Safety and Health. Report PHS-OH-00332, NTIS PB90-100942INZ.

StatSoft, Inc. 2003. *STATISTICA* [data analysis software system], version 6. www.statsoft.com.

Stoeber, W., Flachsbart, H., and Hochrainer, D. 1970. Der Aerodynamische Durchmesser von Latex-aggregaten und Asbestfassern. *Staub-Reinh. Luft* 30:277–285.

Wagner, J. C., Berry, G., Skidmore, J. W., and Pooley, F. D. 1980. The comparative effects of three chrysotiles by injection and inhalation in rats. *IARC Sci Publ.* 30:363–372.

World Health Organization. 1985. *Reference methods for measuring airborne man-made mineral fibres (MMMF)*, WHO/EURO MMMF Reference Scheme prepared by the WHO/EURO Technical Committee for Monitoring and Evaluating Airborne MMMF, Copenhagen.